Available online at www.sciencedirect.com
ScienceDirect
European Polymer Journal 42 (2006) 2931–2939
EUROPEAN POLYMER JOURNAL
www.elsevier.com/locate/europolj

Hyperbranched polyurethane as novel solid–solid phase change material for thermal energy storage

Qi Cao *, Pengsheng Liu *

College of Chemistry, Xiangtan University, Xiangtan 411105, Hunan Province, PR China

Received 23 June 2006; received in revised form 19 July 2006; accepted 21 July 2006

Abstract

A series of novel hyperbranched polyurethane copolymer (HB-PUPCM) using hyperbranched polyester as chain extender was prepared via a two-step process. The phase transition behaviors and morphology of the HB-PUPCM films were investigated using differential scanning calorimetry (DSC), dynamic mechanical thermal analysis (DMA), thermo-gravimetric analysis (TGA), wide-angle X-ray diffraction (WAXD), polarizing optical microscopy (POM) and tapping-mode atomic force microscopy (AFM). HB-PUPCM was proven to a good polymeric solid–solid phase change heat storage material.

Keywords: Hyperbranched polyurethane; Solid–solid phase change material; Polyethylene glycol; Hyperbranched polyester; Micro-phase separation; Heat storage

1. Introduction

Material scientists predicted a prominent role of intelligent materials in the future. In the last few years, this concept has found growing interest as a result of the rise of a new class of materials. They are so-called phase change materials (PCM). PCM are the materials using latent heat to store energy. In recent years, as energy crisis is becoming more and more serious, PCM are attracting lots of attention, a great number of organic, inorganic, polymeric and eutectic PCM have been studied [1–6]. Polyethylene glycol (PEG) has been considered a promising phase-change material for thermal energy storage and temperature control because of its relatively large heat of fusion, congruent melting behavior, noncorrosiveness, and wide melting point range [7]. However, PEG is a classical solid–liquid phase change substance, which must be packaged in special sealed containers to prevent its leakage in the melting state. Thus the high cost of properly packaging PEG restricted its industrial application in the field of thermal energy storage material. Polymeric solid–solid PCM are fairly recently developed functional PCM, which exhibited many desirable characteristics, e.g. no liquid or gas generating, small volume change, no recipient needed to seal them in, being processed into arbitrary shape, even used as a system material directly [7–11], thus it could simplify techniques and reduce cost greatly.

---

* Corresponding authors. Fax: +86 732 8292477.
E-mail addresses: wjcaoqi@163.com (Q. Cao), lpsh@xtu.edu.cn (P. Liu).

0014-3057/$ - see front matter
doi:10.1016/j.eurpolymj.2006.07.020

Chemically cross-linking PEG with high-density polyethylene or encapsulating PEG to make a form-stable particle could retard the flow ability of phase-change material in its molten state [12,13]. But this would simultaneously reduce its heat of fusion and thermal conductivity, with a consequent decrease in the thermal storage and temperature control capabilities of the phase-change material.

Recently new polyurethane systems with hyperbranched polymers attracted an increasing attention [14–16]. They offer an opportunity of modification of the structure of the synthesized materials in a controlled way. However, to the best of our knowledge, PCM polyurethane with hyperbranched polyester as chain extender has never been reported.

In the present paper, the preparation, structural features of the hyperbranched polyurethane with hyperbranched polyester as chain extender and the mechanism of its solid–solid phase change are studied.

2. Experimental

2.1. Materials

Boltorn®H20 (Second generation, $M_w = 1750$ g/mol, hydroxyl number equals 470–500 mg KOH/g, Sweden) was purchased from Perstorp Specialty Chemicals, dried at 60 °C under vacuum for overnight prior to use; Polyethylene glycol (PEG, $M_n = 6000$, from Shantou Guanghua Chemical Reagent Co. Inc., China) was degassed and dried in a round flask under high vacuum (20 Pa) at 100–120 °C for 3–4 h; 4,4′-diphenylmethane diisocyanate (MDI, from Wanhua Chemical Reagent Co. Inc, China) was heated to 60 °C and kept at temperature for 2 h and then filtered through a heated filter. *N*,*N*-dimethylformamide (DMF, from Shantou Guanghua Chemical Reagent Co. Inc., China) was dried by 5 Å molecular sieve for 24 h followed by distillation before use.

2.2. Synthesis of HB-PUPCM

The synthesis route for HB-PUPCM is shown in Scheme 1. The feed ratios for the resulting HB-PUPCM are summarized in Table 1. The general procedure is as follows: Different amounts of dehydrated PEG and excess of MDI in freshly distilled DMF were mixed with stirring in a thermostatic oil-bath at 80 °C under vacuum for 3 h. A predetermined of Boltorn®H20 was dissolved in dried DMF and added to the mixture. After stirring for another 2 h, the reaction mixture was cast in glass pan. Curing was conducted at 80 °C for 24 h, after which the polymer films with a thickness of 0.2–1.0 mm were obtained. The samples were kept in vacuum at room temperature for two weeks before testing.

2.3. Characterization

Dynamic mechanical thermal analysis (DMA) was carried out by Rheometric Scientific DMTA V device with single point bending of 2 mm thick strip at a frequency of 1 Hz and heating rate of 4 °C/min from 0 to 100 °C.

Differential scanning calorimetry (DSC) of the resulting TPU was carried out using a 2920 TA Instrument. Samples (ca. 10 mg) were sealed in aluminum pans and measurements were performed in nitrogen atmosphere at a heating rate of 10 °C/min in the temperature range of −50 to 150 °C. In the first scanning, the sample was heated to 150 °C, kept at this temperature for 5 min, and cooled to −50 °C. In the second scanning, the sample was heated again to 250 °C, and the second scan was recorded. The crystallinity (X_c) of the sample was calculated according to the heat of fusion of the second heat run:

$$X_{\mathrm{C,PEG}}\ (\%) = \frac{\Delta H_{\text{m-PEG}}}{\Delta H^0_{\text{m-PEG}} * \mathrm{SSC}\%} \times 100, \qquad (1)$$

where $\Delta H^0_{\text{m-PEG}} = 197$ J/g is for the 100% crystalline PEG according to Hu et al. [17].

Thermo-gravimetric analysis (TGA) was carried out in Dupont TGA 2950 at a scanning rate of 20 °C/min from 25 °C to 500 °C.

Wide-angle X-ray diffraction (WAXD) was employed for studying the phase morphology by using a Philip PW 1710 at 30 kV and 20 mA. WAXD studies were carried out with samples of 1 mm thickness and with Bragg's angle 2θ from ca. 10 to 50° at the rate of 3°/min.

An observation of polarizing optical microscopy (POM) was performed on a Leitz Laborlux 12POL microscope equipped with a video camera. The sample was placed between a microscope glass and a cover slip and heat with a Leitz 350 hot stage.

Tapping-mode atomic force microscopy (AFM) was used to visualize the images of PU on a DI Nanoscope IIIa AFM, Micro-fabricated cantilevers or silicon probes (Nanoprobes, Digital Instruments)

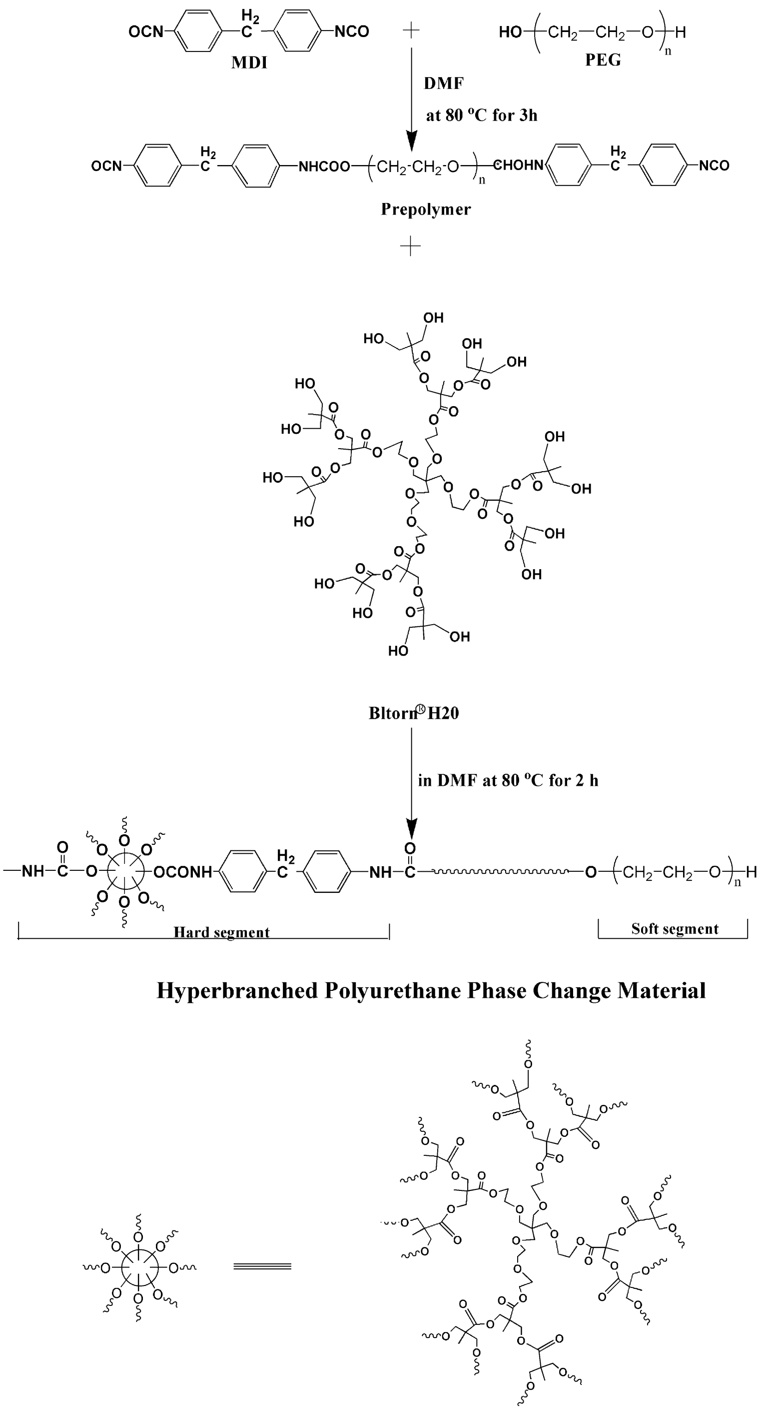

Scheme 1. Synthesis of HB-PUPCM.

with 125 μm long cantilevers were used at their fundamental resonance frequencies, which typically varied from 270 to 350 kHz depending on the cantilever. Cantilevers had a very small tip radius of 5–10 nm. The AFM was operated at ambient with a double-vibration isolation system. Extender electronics were used to obtain height information simultaneously. The lateral scan frequency was about 1.5 Hz.

Table 1
Synthesis parameters for HB-PUPCM with different compositions

Soft segment (M_n, g mol^{-1})	Chain extender	[NCO]/[OH][a]	SSC[b] (wt.%)
PEG6000	H20	1.00	90
PEG6000	H20	1.00	80
PEG6000	H20	1.00	70
PEG6000	H20	1.00	60

SSC: Soft segments content.

[a] Feed molar ratio of isocyanate groups to hydroxyl groups.

[b] Calculated according the feed weight ratio: [SSC% = $W_{PEG}/(W_{MDI} + W_{H20} + W_{PEG})] \times 100$.

3. Results and discussion

3.1. Investigation of thermal property

Fig. 1 shows the DMA curves of a sample HB-PUPCM with 80% PEG soft segments content (SSC%). The peak in the tan δ curve and the rapid shift of the E' curve indicate that melting has occurred, where the enthalpy is 118.1 J/g according to DSC measurement (Table 1). In contrast with pure PEG, PEG in HB-PUPCM does not change to the liquid state even at a temperature much higher than the melting point of pure PEG. The DMA curve shows that PEG segments in the HB-PUPCM remain in the solid state even when the temperature rises to 100 °C, over 33 °C above the melting point of pure PEG. These features imply that the hard segment domain served as skeleton which restricts the free movement of the soft PEG segments at temperature above PEG's melting point, so that HB-PUPCM still keep in solid state.

Fig. 2 shows the DSC traces of pure PEG6000 and HB-PUPCM. The DSC measurement of HB-PUPCM with 80% SSC shows heat absorption at about 66.39 °C, in the heating cycle, indicating that there is a phase transition having taken place. This should be a solid–solid phase transition, since the sample has not melted to a liquid at that time, as indicated by the DMA analysis above.

Five HB-PUPCM samples with different SSC% were analyzed using DSC. The relationship between the phase transition temperature, the enthalpies, the X_C and the soft segment contents are summarized in Table 2. The enthalpies calculated from DSC plots decrease with decreasing soft segment content. HB-PUPCM samples are copolymer where only PEG segments are crystalline, it is possible that the ΔH_m decreases with the decreasing of PEG%; but the crystallinity of PEG segments in the copolymer does not change much. At the same time, we could find that the changes of phase transition temperatures have the similar rules as the enthalpies. The phase transition temperatures fall down as the weight percentages of PEG decline. The reason is discussed as follows. The hard segment in HB-PUPCM can destroy the perfection of the crystallization. So the defects of crystal lattices increased with the increase of the hard segment, which cause the crystals can be damaged at lower temperature.

It is evident that the SSC% has influence on phase transition temperature of the soft segments;

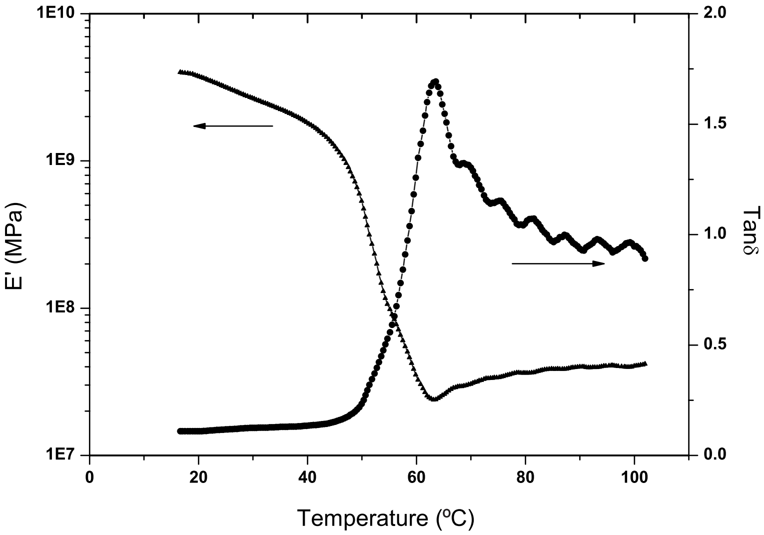

Fig. 1. Storage modulus (E') and tan δ of HB-PUPCM with various wt.% of hard segment as a function of temperature.

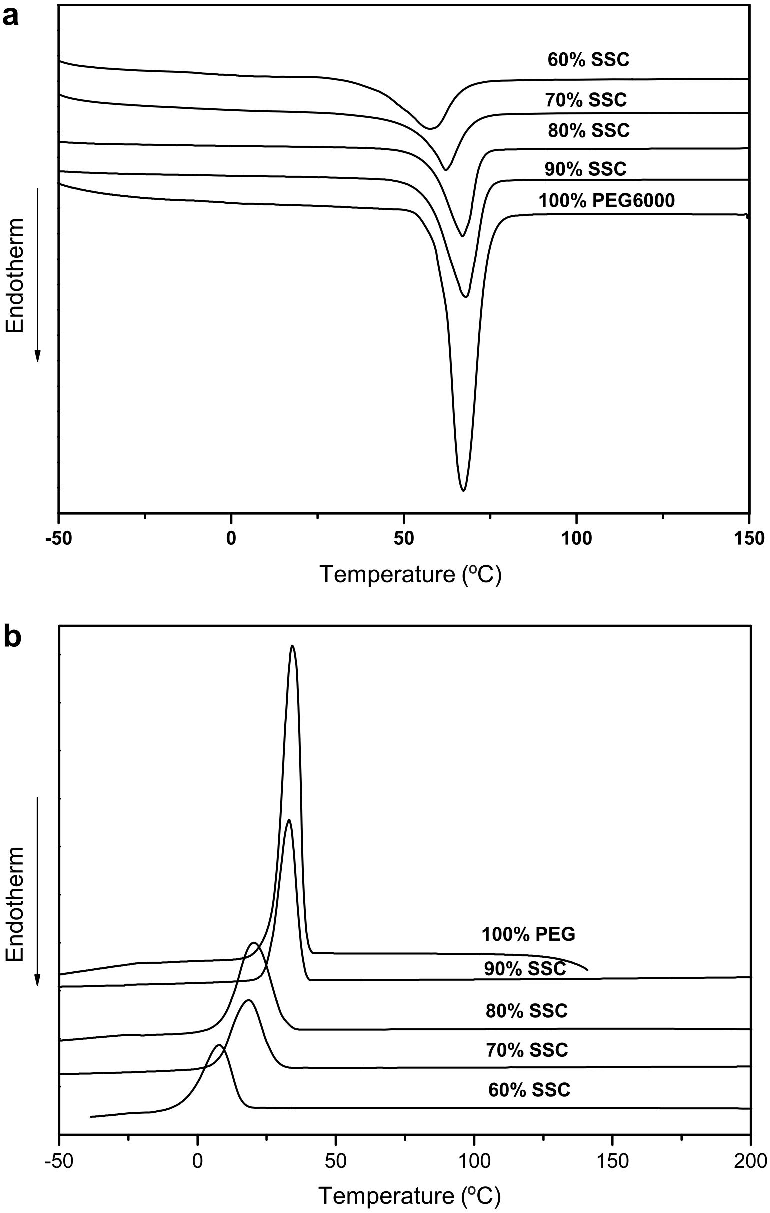

Fig. 2. DSC traces for pure PEG6000 and HB-PUPCM: (a) heating traces; (b) cooling traces.

Table 2
Thermal properties of PEG6000 and HB-PUPCM measured by DSC analysis

Samples	Phase transition	$\Delta \mathrm{H_m}$[a] (J/g)	T_m[a] (°C)	ΔH_c[a] (J/g)	T_c[a] (°C)	X_C (%)	T_1[b] (°C)	T_2[b] (°C)
PEG6000	Solid–liquid	155.1	67.2	152.0	34.6	78.7	–	–
90% SSC	Solid–solid	138.2	67.0	132.3	33.2	77.9	317.6	399.1
80% SSC	Solid–solid	118.1	66.4	115.8	20.4	74.9	318.1	406.5
70% SSC	Solid–solid	102.8	62.2	100.9	18.6	74.5	320.3	412.8
60% SSC	Solid–solid	91.2	57.5	89.4	7.8	77.1	334.1	418.7

[a] The data of heating run was obtained according to the second DSC heating scan of HB-PUPCM.

[b] Peak temperature obtained from DTG curves.

Table 3
Properties of HB-PUPCM with 100 heating–cooling thermal cycles

	ΔH_m (J/g)	T_m (°C)	Phase transition
Un-cycled	138.2	67.05	Solid–solid
Cycled	137.8	66.93	Solid–solid

but the phase transition behavior of crystallites was less pronounced as decreasing the soft segments of HB-PUPCM. The samples with higher percentage of soft segment showed rather more heat of transition at the melting temperature, suggesting that more ordered polymer package was obtained at high percentage of PEG soft segment. Viewing from the microcosmic level, in the process of phase transition of HB-PUPCM, with the temperature increasing, the molecular thermal movement of PEG soft segment is quickening. It breaks away from the bandage of intermolecular force. The crystalline perfection of PEG has been destroyed. So it turns into amorphous state. But the amorphous

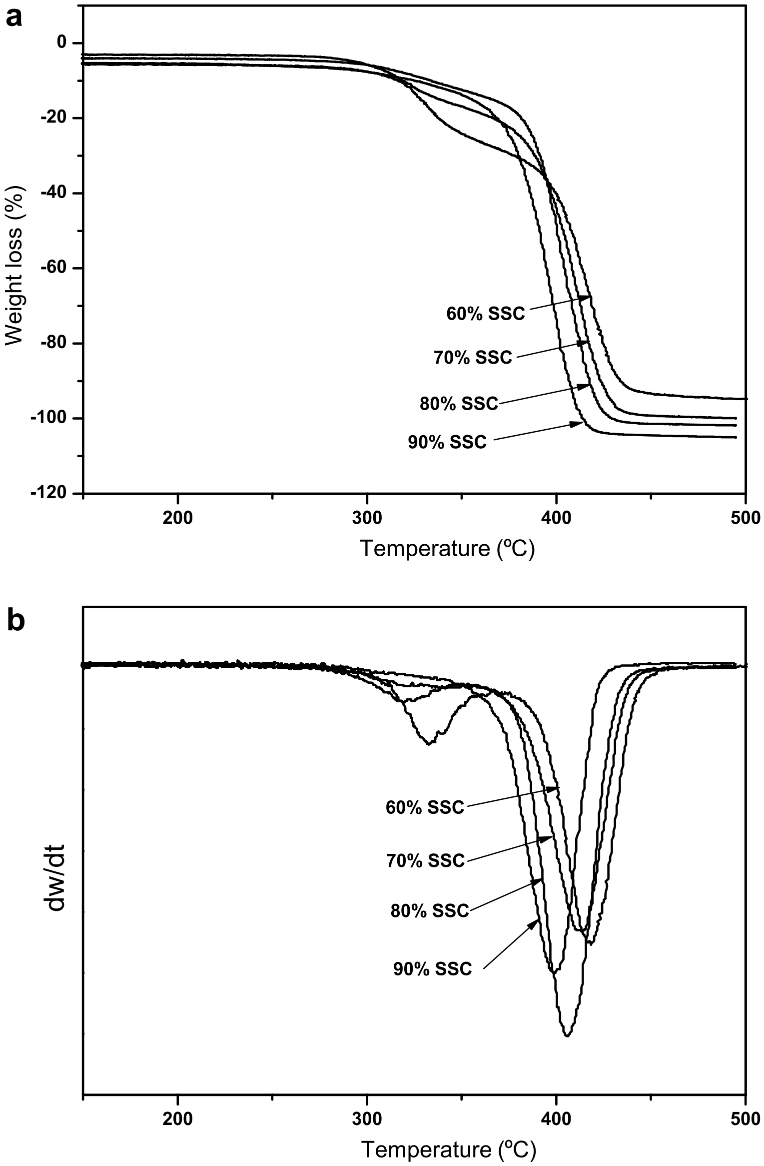

Fig. 3. Thermo-gravimetric analysis (TGA) of HB-PUPCM with various soft segment contents in N_2: (a) TGA thermogram curves; (b) TGA thermogram derivative curves.

PEG is connected with the hard segment. It can only vibrate and rotate, but cannot translate freely. It shows a special solid–solid phase change behavior. So we can come to a conclusion that solid–solid phase change of HB-PUPCM is the soft segment PEG's transition from a crystalline solid state to an amorphous solid state essentially. The energy is mainly obtained from the heat coursed by entropy change between the low entropy crystal state and high entropy amorphous state.

Table 3 shows the thermal properties of HB-PUPCM with 80 SSC% after undergoing the heating–cooling cycle 100 times. Being subjected to this heating and cooling 100 times did not change the phase-change behavior, enthalpy, and phase-change temperature of the sample, confirming the thermal stability of the HB-PUPCM as a solid–solid phase transition material.

At high temperature, polyurethane underwent degradation first via decomposition of urethane bonds, followed by breakage of the soft segment phase [18,19]. Such degradation process could be easily monitored by thermo-gravimetric analyses (TGA) [20]. The thermal stability of PEG based HB-PUPCM with different SSC% was also investigated by TGA. The TGA thermograms are illustrated in Fig. 3 and the results are summarized in Table 2. The degradation of HB-PUPCM is a two-step process under the protection of nitrogen. These degradation processes are clearly demonstrated in the thermogram derivative curves illustrated in Fig. 3(b). It is noted that the first degradation temperature (T_1) and the distinct degradation temperature (T_2) of the HB-PUPCM all increase with decreasing PEG content, and confirming the thermal stability of the HB-PUPCM.

3.2. Crystalline morphology investigations

To reveal the morphology of HB-PUPCM, WAXD patterns of pure PEG6000 and HB-PUPCM are shown in Fig. 4. It is obvious seen that pure PEG and HB-PUPCM show similar diffraction curves on which diffraction angle and crystal plane distance are nearly the same. It implies that they have the same crystal structure and unit cell type. In other words, crystal structure of PEG has not changed by the procedure of polymerization. The HB-PUPCM shows a lower diffraction peak height and broader half-width pure PEG, which indicates that its crystal particles of HB-PUPCM are smaller and the crystallinity decreases.

The crystallization of soft segments was disturbed pronouncedly in the PU, due to the hindrance of hard segments [21]. As shown in Fig. 4, very similar diffraction curves appear for all polyurethane with various PEG SSC%, however the intensity gradually decreases as decreasing the SSC%. These suggest that the PEG in pure PEG and HB-PUPCM have same crystal structure. The

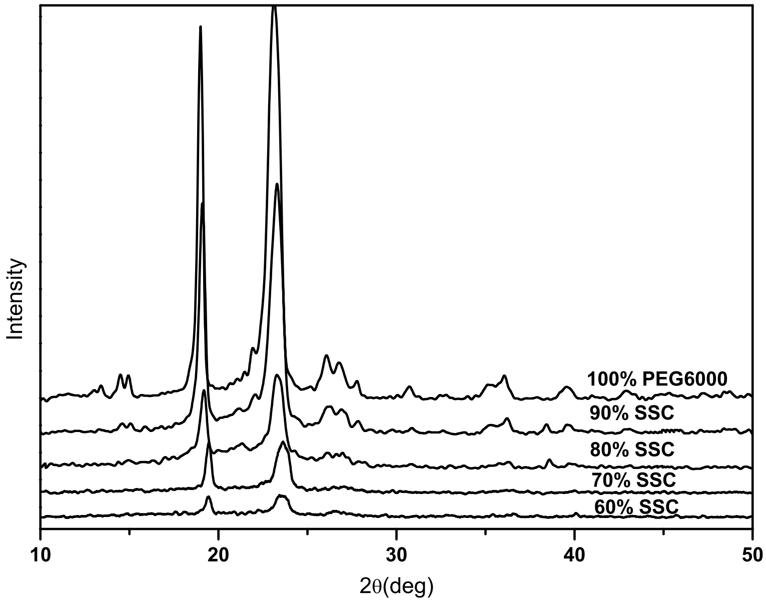

Fig. 4. WAXD profiles of the pure PEG6000 and HB-PUPCM with various soft segment contents.

crystallization of PEG segments in the HB-PUPCM was disturbed by the hard segment, which results in the crystallinity of PEG segments decreases with the increasing of percentage of hard segment in the HB-PUPCM. These results are in good agreement with the DSC results discussed above.

POM micrographs of pure PEG with Mn of 6000 and HB-PUPCM at 200 magnifications are showed in Fig. 5(a) and (b). It is observed that both resultant micrographs show obvious cross extinction patterns, which is an indication that both of them are crystalline and their crystal structures are spherulite. In other words, crystal structure of PEG has not changed by the procedure of polymerization. But the spherulites size of HB-PUPCM is much smaller than that of PEG, it indicates that the hard segment confines the crystallization of PEG in HB-PUPCM, and the crystalline perfection of PEG has been destroyed.

To investigate the morphology in the transition process, micro-morphology is recorded by POM in a heating process. Under the transition temperature, the spherulite has no change with the temperature increasing; the spherulite starts to be destroyed when the temperature reaches transition temperature. At last, the spherulite structure is destroyed completely, and the visual field of POM is dark, but no liquid is observed at the heating process, which is indicated that the PEG soft segment has been transferred from crystal solid to amorphous solid. The transition is also proved to be a solid–solid phase change.

AFM has been proved to be a valuable tool for evaluating the surface features of the PU materials and compositions in the surface topography. Fig. 6 shows AFM images for HB-PUPCM with 70% and 80% PEG SSC respectively. The surface roughness of both samples is measured and found

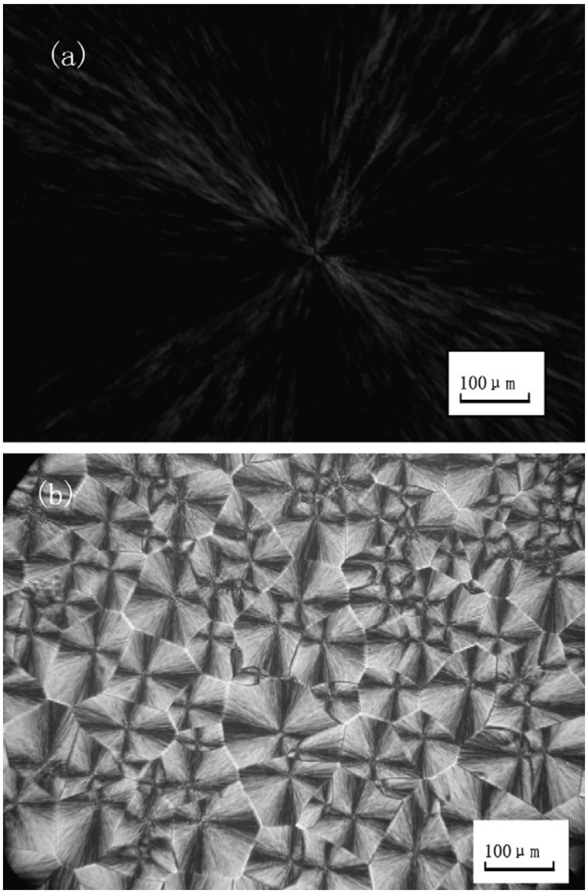

Fig. 5. POM of samples: (a) PEG 6000 (at room temperature) (b) HB-PUPCM (at room temperature).

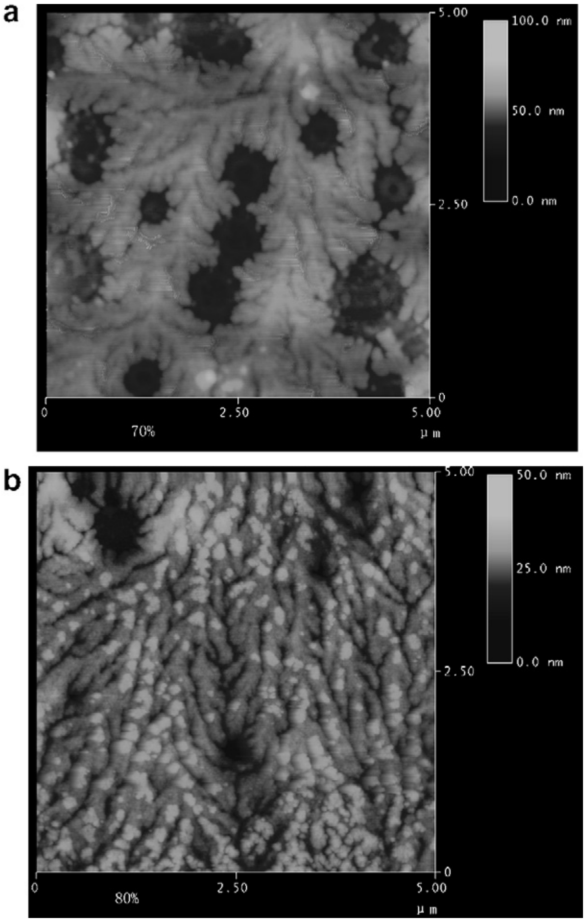

Fig. 6. AFM height images of HB-PUPCM films illustrating surface morphological changes resulting from different SSC%.

to be 100 nm for (70% SSC) and 50 nm for (80% SSC). The hard segment domains in (70% SSC) are larger than that in (80% SSC).

For a moderate force image, the high height corresponded to low modulus; therefore, the lighter height image was richer in polyurethane, while the darker height image corresponded to the hard segment. We used a conventional interpretation of modulus-sensitive height images at light tapping where the lighter color portions were assigned to the crystallites of PEG soft segments. The AFM image reveals the connected PEG soft segment domains. Importantly, the AFM image of HB-PUPCM showed the existence of crystallites. This was in general agreement with the DSC, WAXD and POM results. The crystallization of the PEG was disturbed with the increase of hard segment content in the HB-PUPCM.

In Fig. 6, spherical phases in (70% SSC) can be observed that separate from the continuous phase. The spherical phase is attributed to the MDI-H20 aggregate. On the other hand, the AFM micrograph of the HB-PUPCM with 80% SSC showed a more continuous structure. Therefore, from the AFM result, it also can be concluded that the PEG containing segmented polyurethane with low PEG content forms a spherical morphology (hard segment domains). On the other hand, a co-continuous morphology forms when the PEG content is high ($\geqslant$80%).

4. Conclusions

The HB-PUPCM possessed typical solid–solid phase transition property. The reversible phase transition between amorphous and crystalline of the soft PEG segment accounted for the good energy storage behavior of HB-PUPCM. The hard segment in HB-PUPCM, severing as skeleton, restricted the free movement of the molecular chain of PEG at high temperature, thus HB-PUPCM could keep its solid state in the transition processing. The latent heats, phase transition, and thermal stable property of HB-PUPCM could be adjusted through the control of the proportion of components. By changing the weight percentage of PEG, the HB-PUPCM would have different enthalpies and different transition temperature. HB-PUPCM could be used as a new kind of solid–solid phase change materials for thermal energy storage and temperature control. It has a great potential for thermal energy storage applications.

References

[1] Abhat A. Low temperature latent thermal energy storage system: heat storage materials. Sol Energ 1983;30:313–32.

[2] Kaygusuz K. The viability of thermal energy storage. Energ Source 1999;21:745–56.

[3] Mohammed MF, Amar MK. A review on phase change energy storage: materials applications. Energ Convers Manage 2004;45:1597–615.

[4] Feldman D, Banu D, Hawes D. Low chain esters of stearic acid as phase change materials for thermal energy storage. Solar Energ Mater 1995;36:311–22.

[5] Sari A, Kaygusuz K. Thermal performance of myristic acid as a phase change material for energy storage application. Renew Energ 2001;24:303–17.

[6] He Q, Zhang W. A study on latent heat storage exchangers with phase-change material. Int J Energ Res 2001;25:331–41.

[7] Jiang Y, Ding EY, Li GK. Study on transition characteristics of PEG/CDA solid–solid phase change materials. Polymer 2002;43:117–22.

[8] Liang XH, Guo YQ. Crystalline–amorphous phase transition of a poly(ethylene glycol)/cellulose blend. Macromolecules 1995;28:6551–5.

[9] Zhang M, Na Y, Zhenhua Jiang. Preparation and properties of polymeric Solid–solid phase change materials of polyethylene glycol (PEG)/poly(vinyl alcoho1) (PVA) copolymers by graft copolymerization. Chem J Chin Univ 2005;26:170–4.

[10] Ye Hong, Ge Xin-shi. Preparation of polyethylene-paraffin compound as a form-stable solid–liquid phase change material. Sol Energ Mater Sol Cells 2000;64:37–44.

[11] Haws DW, Banu D, Feldma D. Latent heat storage in concrete. II. Sol Energ Mater 1990;21:61–80.

[12] Sayler I. Vol, O. Griffen. US. Patent 4,825,939;1989.

[13] Sayler I. Vol, O. US. Patent 4,711,813;1987.

[14] Jahromi S, Litvinov V, Coussens B. Polyurethane networks bearing dendritic wedges: synthesis and some properties. Macromolecules 2001;34:1013–7.

[15] Nasar AS, Jikei M, Kakimoto M. Synthesis and properties of polyurethane elastomers crosslinked with amine-terminated AB2-type hyperbranched polyamides. Eur Polym J 2003;39:1201–8.

[16] Okrasa L, Zigon M, Zagar E, Czech P, Boiteux G. Molecular dynamics of linear and hyperbranched polyurethanes and their blends. J Non-Cryst Solids 2005;351:2753–8.

[17] Hu Y, Rogunova M, Topolkaraev V, Hiltner A, Baer E. Aging of poly(lactide)/poly(ethylene glycol) blends. Part 1. Poly(lactide) with low stereoregularity. Polymer 2003;44:5701–10.

[18] Yang WP, Macosko CW, Wellinghoff ST. Thermal degradation of urethanes based on 4,4′-diphenylmethane diisocyanate and 1,4-butanediol(MDI/BDO). Polymer 1986;27:1235–40.

[19] Petrovic ZS, Zavargo Z, Flynn JH, Macknight WJ. Thermal degradation of segmented polyurethanes. J Appl Polym Sci 1994;51(6):1087.

[20] Asim P, Sadhan CJ. Properties of bulk-polymerized thermoplastic polyurethane nanocomposites. Polymer 2005;46:3394–406.

[21] Blackwell J, Gardner KH. Structure of the hard segments in polyurethane elastomers. Polymer 1979;20:13.